

PHOTOCHEMISTRY

Mechanism of Exciplex Decay: The Quantum Yields and the Rate Constants of Radical Ion Formation from Exciplexes with Partial Charge Transfer

D. N. Dogadkin*, E. V. Dolotova*, I. V. Soboleva*, M. G. Kuzmin*,¹ V. F. Plyusnin**, I. P. Pozdnyakov**, V. P. Grivin**, E. Vauthey***, P. Brodard***, and O. Nicolet***

*Moscow State University, Moscow, 119992 Russia

**Institute of Kinetics and Combustion, Siberian Division, Russian Academy of Sciences, ul. Institutskaya 3, Novosibirsk, 630090 Russia

***University of Geneva, 30 quai Ernest-Ansermet, Geneva 4, CH-1211, Switzerland

Received April 28, 2004

Abstract—The dynamics of exciplex and radical ion formation was studied in donor–acceptor systems with $\Delta G_{\text{et}}^* > -0.1$ eV. It was shown that the quenching of excited singlet states of aromatic molecules by electron donors in polar solvents led to the formation of radical ions via exciplex dissociation resulting to complete charge separation. Intersystem crossing and internal conversion into the ground state (back electron transfer) compete with this process. The quantum yields and the rate constants of the radical ion formation were measured.

In the previous work [1], we studied the processes of intersystem crossing for a series of donor–acceptor systems giving exciplexes with partial charge transfer. It was shown that the fluorophore triplet state was formed via intersystem crossing not only from the excited singlet state of the molecule, but also from the corresponding exciplex in the range of the solvent permittivity of $\epsilon = 2$ –38. In this work, we studied another channel of transformation of exciplexes with partial charge transfer, the dissociation into radical ions observed in rather polar solvents ($\epsilon > 20$). Depending on the mechanism of photoinduced electron transfer and solvent polarity, radical ions can be formed either directly in the coupling of excited acceptor with electron donor molecules or as a result of exciplex dissociation [2–8].

Donor–acceptor systems were selected to have the Gibbs energy of electron transfer ΔG_{et}^* ranging from -0.1 to $+0.1$ eV (Table 1). In these systems, exciplexes are formed in both polar and nonpolar solvents with almost diffusion-controlled rate constants. In this work, were recorded the absorption spectra of transient species and measured the quantum yields and the rate constants of radical ion formation using the techniques of time-resolved ps, ns, and μs spectroscopy.

EXPERIMENTAL

The procedures of purification of the substances used (electron acceptors: 9-cyanoanthracene (CA), 9-cyanophenanthrene (CP), and 1,12-benzperylene (BP);

electron donors: 1,2-dimethoxybenzene (12DMB), 1,3,5-trimethoxybenzene (135TMB), 1,2,3-trimethoxybenzene (123TMB), and 1,8-dimethylnaphthalene (18DMN); and solvents: toluene (PhCH_3), butyl acetate (AcOBu), butyronitrile (PrCN), and acetonitrile (MeCN)), experimental conditions and data processing of the fluorescent measurements were described elsewhere [9–11].

To measure transient spectra on the ps time-scale, the diffraction of a probing pulse of light continuum on an induced grating (transient grating spectroscopy) was used [4, 12]. Samples were excited by the third harmonics of a Nd : YAG laser at the wavelength of 355 nm with a pulse energy of 10 mJ. The spectrum of the probing pulse in the first diffraction order was recorded by a spectrograph and a CCD camera.

The absolute quantum yield of radical ions was determined by measuring photocurrent after a laser pulse in an electrochemical cell and from absorption spectra on the ns and μs time-scales. Equipment for the measurement of pulsed photocurrent generated in solutions of donor–acceptor systems as a result of the formation of free ions from radical ion pairs was described in [13]. For the generation of transient species, frequency-tripled (355 nm) pulses from a Nd : YAG laser were also used in this case. In order to measure the quantum yield of radical ions (ϕ_{R}), the benzophenone–diazabicyclo[2.2.2]octane (Ph_2CO –DABCO) system with a quantum yield of 1 [14] was used as a reference. The DABCO concentration was 0.02 mol l^{-1} . The absorbance of Ph_2CO and of the electron acceptor was

¹ E-mail: kuzmin@photo.chem.msu.ru

Table 1. The absolute quantum yields of radical ions (ϕ_R), the quantum yields of radical ions (ϕ_R^0) from exciplexes, and the rate constants of radical ion formation from exciplexes (k_R') for the systems under study

System (ΔG_{et}^* , eV)	H_{12}	(μ_0^2/ρ^3)	$H_{22}^0 - H_{11}^0$	Solvent	[D], M	τ_0' , ns	$1 - \phi_f/\phi_f^0$	ϕ_R	ϕ_R^0	k_R' , μs^{-1}
CA – 135TMB (0.09)	0.28	1	0.4	MeCN	0.069	1.1	0.9	0.048 ^a	0.055	50
				PrCN	0.071	0.8	0.8	0.009 ^a	0.012	14.6
BP – 124TMB (–0.01)	0.44	1	0.13	MeCN	0.3	10 [8]	0.996	0.53 ^a	0.53	53
				PrCN	0.3	15 [8]	0.98	0.18 ^a	0.18	12
CP – 135TMB (–0.02)	0.2	0.72	–0.13	PrCN	0.061	14	0.6	0.12 ^b	0.2	14.3
					0.110		0.7	0.14 ^b		
					0.151		0.8	0.16 ^b		
					0.388		0.9	0.19 ^a		
CP – 12DMB (–0.06)	0.2	0.7	–0.3	PrCN	0.319	8	0.98	0.5 ^a	0.59	74
CP – 123TMB (–0.09)	0.2	0.5	–0.55	PrCN	0.035	2.3	0.7	0.12 ^b	0.18	78.2
					0.067		0.8	0.16 ^b		
					0.110		0.9	0.14 ^b		
CA – 18DMN (–0.1)	0.42	0.7	0.3	MeCN	0.27	13	0.97	0.81 ^a	0.83	63.8
				PrCN	0.236	34	0.93	0.22 ^a	0.24	7.1

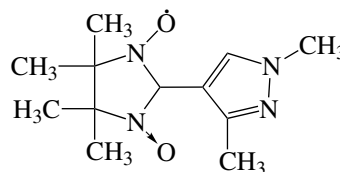
^a Determined by photocurrent measurements. ^b Determined from the absorption spectra of the $CP^{\bullet-}$ radical anion.

0.5 at the excitation wavelength of 355 nm. The donor concentration selected was such that the degree of fluorescence quenching was not less than 0.8–0.9.

The recording of transient absorption spectra on ns and μs time-scales and a corresponding laser pulse photolysis setup were described in [1, 15]. An excimer XeCl laser with emission at the wavelength of 308 nm and a pulse energy of 10 mJ was used.

The molar decadic absorption coefficient of the $CP^{\bullet-}$ radical anion in butyronitrile at $\lambda_{max} = 410$ nm of the absorption band, $\epsilon_{410}(CP^{\bullet-})$, was determined with the use of the reaction of $CP^{\bullet-}$ with the stable nitroxyl radical RA-21 (arbitrary designation) of the structure given in Fig. 1. The synthesis and the optical parameters of this and similar radicals are given in [16]. We already used RA-21 for the determination of the molar decadic absorption coefficients of several sulfur-containing radicals [17]. The absorption bands of the RA-21 nitroxyl radical have maximums at 347 ($\epsilon_{347}(RA-21) = 13800$ l mol⁻¹ cm⁻¹) and 600 nm ($\epsilon_{600}(RA-21) \approx 1000$ l mol⁻¹ cm⁻¹) and is convenient for the purpose, because it does not react with CP in the ground state, but interacts with the radical anion $CP^{\bullet-}$ at a high rate constant ($k = 2.6 \times 10^9$ l mol⁻¹ s⁻¹); weakly

absorbs at 308 nm ($\epsilon_{308}(RA-21) \approx 2000$ l mol⁻¹ cm⁻¹); is stable under exposure to laser irradiation; and practically does not absorb in the range of the absorption bands of $CP^{\bullet-}$ and 3CP (400–500 nm). The absorbance amplitude at 410 nm (the band of the $CP^{\bullet-}$ radical) after the laser pulse and the amplitude and clarification kinetics (decay of optical absorption) at 347 nm (the absorption band of RA-21) were measured for the solutions containing RA-21 as a function of the laser pulse intensity. The extrapolation to zero intensity [17] and zero initial concentration of $CP^{\bullet-}$ allowed us to determine the value $\epsilon_{410}(CP^{\bullet-}) = 19700 \pm 400$ l mol⁻¹ cm⁻¹.

**Fig. 1.** Structure of the RA-21 nitroxyl radical.

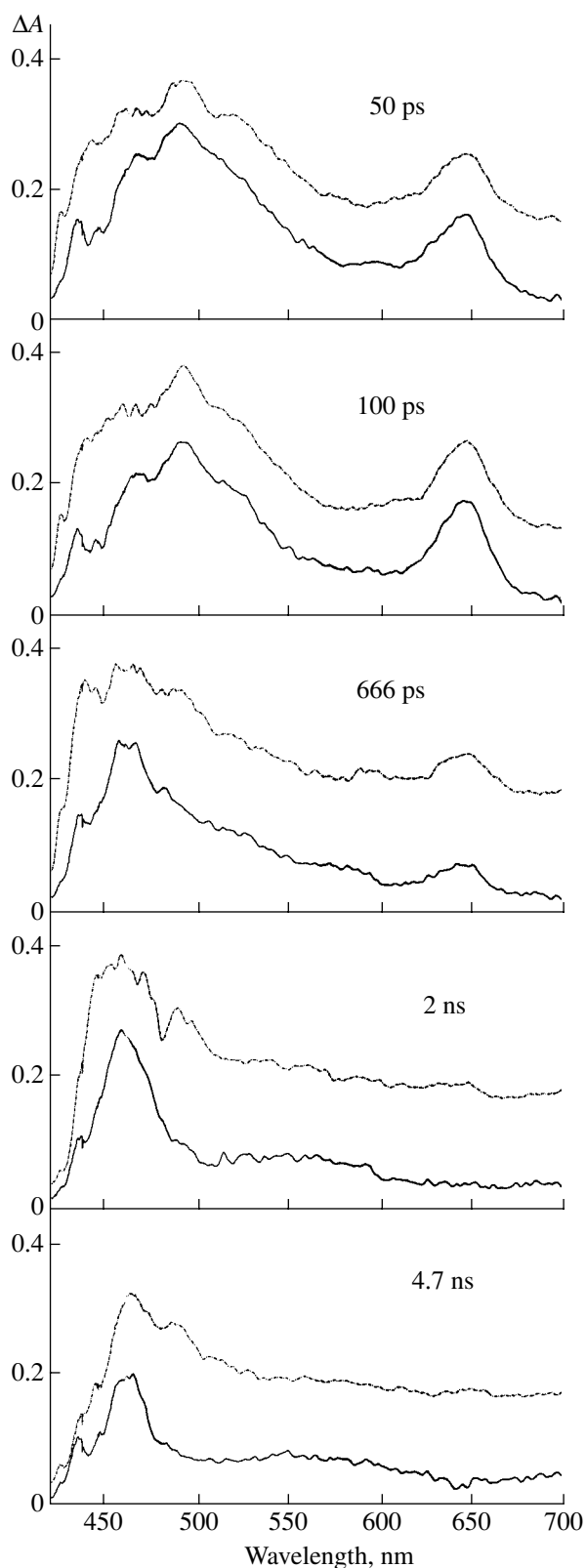


Fig. 2. Transient-grating spectra of CP in the presence of 12DMB (0.3 mol l^{-1}) in PrCN (solid lines) and AcOBu (dashed lines). The degree of quenching of CP fluorescence was 0.98 in PrCN and 0.9 in AcOBu. The delay time is specified in the plot.

To determine the overall quantum yield ϕ_R of the $\text{CP}^{\cdot-}$ radical anion, the T–T absorption band (431 nm) of anthracene in benzene was used as a reference for measuring the laser pulse intensity [18, 19].

The quantum yield ϕ_R was calculated by the following expression:

$$\phi_R = \phi^0(^3\text{An})\varepsilon_{431}(^3\text{An})\Delta A_{410}(\text{CP}^{\cdot-}) / \varepsilon_{410}(\text{CP}^{\cdot-})\Delta A_{431}(^3\text{An}), \quad (1)$$

where $\phi^0(^3\text{An}) = 0.75$ is the quantum yield of intersystem crossing of anthracene, $\varepsilon_{410}(\text{CP}^{\cdot-})$ and $\varepsilon_{431}(^3\text{An}) = 69000 \text{ l mol}^{-1}\text{cm}^{-1}$ [18, 19] are the absorption coefficients at the bands of the $\text{CP}^{\cdot-}$ radical anion and anthracene in the triplet state, $\Delta A_{431}(^3\text{An})$ and $\Delta A_{410}(\text{CP}^{\cdot-})$ are the absorbances at maximum of these bands.

RESULTS

Transient-grating (TG) spectra on ps time scale make it possible to reveal the character of primary processes occurring in an acceptor–donor–solvent system. An appearance of the bands corresponding to the absorption of the excited singlet state of fluorophore and an increase in their intensity are observed during the first 50–100 ps after the laser pulse (Figs. 2, 3). The further increase in the delay time of the probing pulse results in a decrease in the intensity of these bands with a simultaneous increase in the intensity of exciplex absorption, which is superposition of the absorption bands of corresponding radical cations and anions [20].

The TG spectra observed upon excitation of CP in the presence of 0.3 mol l^{-1} of 1,2-dimethoxybenzene (12DMB) in PrCN and AcOBu are given in Fig. 2. The absorption bands with maximums at 647 nm and in the range of 500–520 nm were attributed to the $S_n \leftarrow S_1$ absorption of CP, because they completely disappear during the time less than 2 ns (when the quenching degree is higher than 0.9, the lifetime of $^1\text{CP}^*$ is less than 2 ns). The increasing absorption with maximums at 430 and 465 nm corresponds to the CP–12DMB exciplex formed and coincides with the absorption spectrum of $\text{CP}^{\cdot-}$ [1]. According to published data, the absorption of the radical cation of 12DMB $^{\cdot+}$ is observed in the range shorter than 430 nm with a maximum at 407 nm [21], which is beyond the limits of measurement of the equipment used. Note that the T–T absorption band of ^3CP with a maximum at 485 nm observed on the μs time-scale is almost undetectable in the TG spectra, because the measurement time range ($<5 \text{ ns}$) is significantly shorter than the CP–12DMB exciplex lifetime (8 ns in PrCN and 36 ns in AcOBu).

[22] and, consequently, than the time of the formation of the CP triplet state from the exciplex.

The TG spectra of 1,12-benzoperylene (BP) in the presence of 1,2,4-trimethoxybenzene (124TMB) in MeCN and AcOBu are given in Fig. 3. The initially observed absorption band with a maximum at 520 nm corresponds to the $S_n \leftarrow S_1$ absorption of BP [23]. The broad band with maximums at 545, 530, 515, and 470 nm coincides with the absorption spectrum of the $BP^{\cdot-}$ radical anion [8, 21] and belongs to the absorption of the exciplex formed. The absorption by the radical cation of $124TMB^{\cdot+}$ contributes slightly into the overall absorption at $\lambda = 450$ nm [24]. The T-T absorption band, which is observed in the wavelength range of 455–470 nm [8, 19], does not manifest itself in these spectra. This is also due to the fact that the exciplex lifetime (10 ns in MeCN [8]) is longer than the time of TG spectral measurements.

The transient absorption spectra observed upon CP excitation in butyronitrile in the presence of 135TMB and 123TMB on ns and μ s time scales are given in Fig. 4. The band with a maximum at 485–490 nm corresponds to the T-T absorption of the CP triplet state [1]. The bands with maximums at 430 and 575 nm, the intensity of which increases with an increase in the concentration of 135 TMB, belong to the absorption of the $CP^{\cdot-}$ radical anion and 135TMB radical cation, respectively [1]. In the CP–123TMB system, the absorption band of $CP^{\cdot-}$ overlaps the $123TMB^{\cdot+}$ absorption band with a maximum at 420 nm— $\epsilon_{420}(123TMB^{\cdot+}) = 2800 \text{ l mol}^{-1} \text{ cm}^{-1}$ [24], which is much lower than $\epsilon_{410}(CP^{\cdot-}) = 19700 \text{ l mol}^{-1} \text{ cm}^{-1}$. Therefore, the $123TMB^{\cdot+}$ absorption makes an insignificant contribution to the overall absorption at 420 nm at the initial point of time. However, the band of $123TMB^{\cdot+}$ becomes detectable at times exceeding one μ s, because radical cations of aromatic compounds decay more slowly than radical anions.

Thus, absorption due to the fluorophore excited singlet state and the exciplex is observed within a time range less than 5 ns, while the T-T absorption bands of 3CP and of free radical ions are observed at a time longer than 50 ns.

DISCUSSION

The TG spectra of transient species observed allowed us to establish the dynamics of exciplex and radical ion formation in the systems under consideration. In butyl acetate, the solvent of low polarity, the formation of free radical ions does not occur, and the TG spectra of the systems of interest are the combination of the absorption bands of the excited singlet state of fluorophore and exciplex.

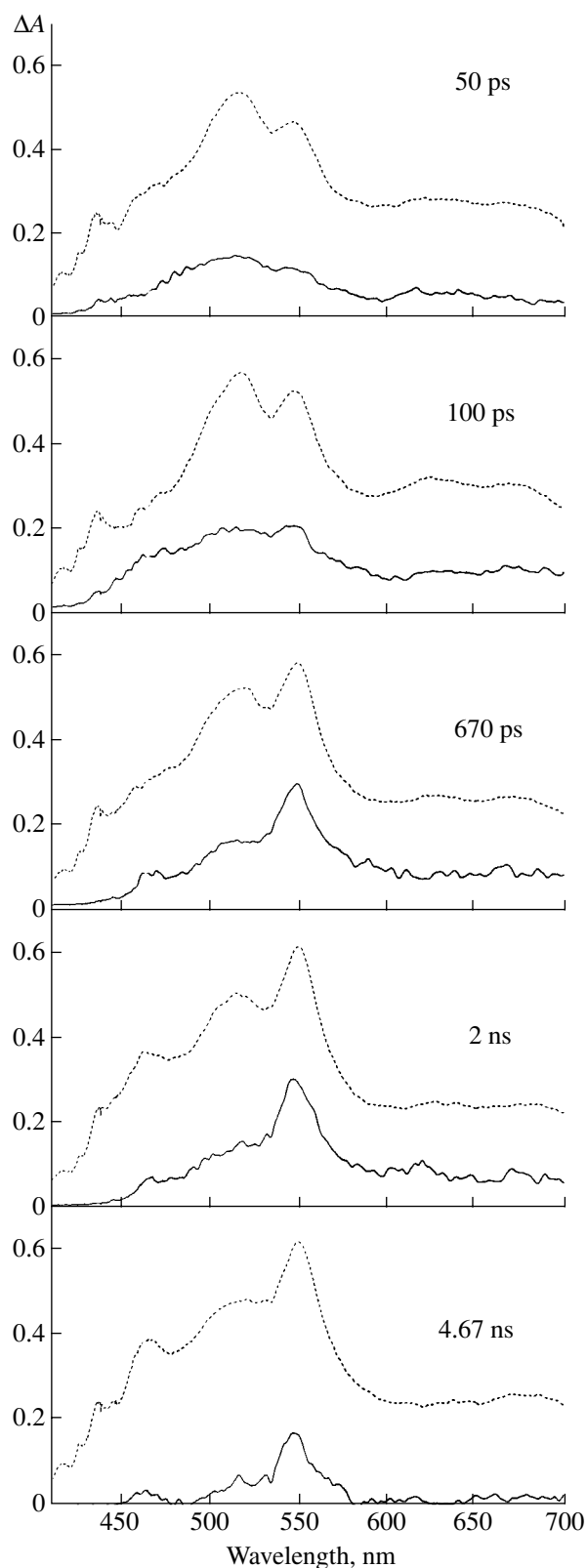


Fig. 3. Transient-grating spectra of BP in the presence of 124TMB (0.3 mol l^{-1}) in MeCN (solid lines) and AcOBu (dashed lines). The degree of quenching of BP fluorescence was 0.99 in MeCN and 0.8 in AcOBu. The delay time is specified in the plot.

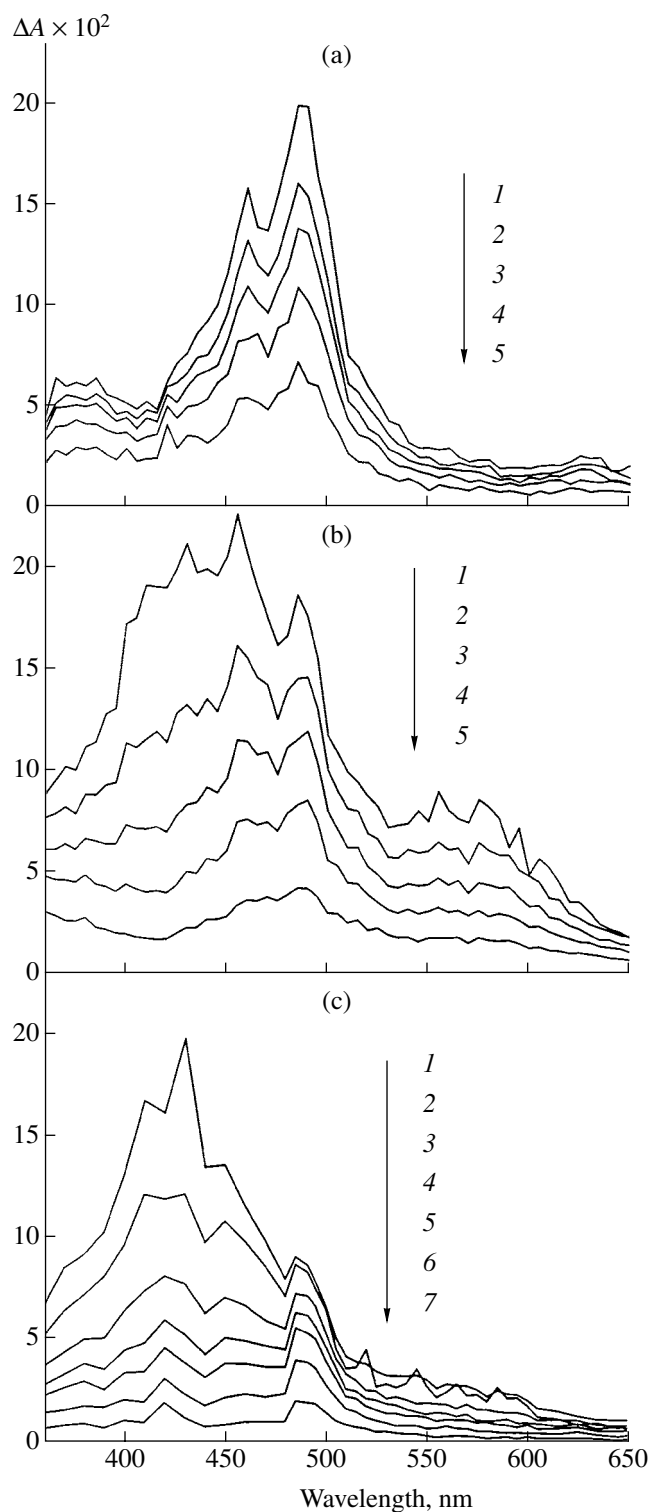


Fig. 4. Spectra of transient absorption observed in the laser pulse photolysis (308 nm) of CP in butyronitrile in the absence and in the presence of electron donors. (a) CP in the absence of a donor, time after the laser pulse in μs : (1) 0, (2) 1.2, (3) 2.4, (4) 4.0, and (5) 8.0. (b) CP + 0.151 mol l^{-1} 135TMB, time after the laser pulse in μs : (1) 0, (2) 0.8, (3) 2.0, (4) 4.0, and (5) 10.0. (c) CP + 0.067 mol l^{-1} 123TMB; time after the laser pulse in μs : (1) 0, (2) 0.4, (3) 1.2 (4) 2.0, (5) 2.8, (6) 4.8, and (7) 10.0.

In polar solvents, the generation of radical ions may occur according to two mechanisms, either by outer-sphere electron transfer directly as a result of the interaction of a donor and an acceptor in the excited state or by exciplex dissociation. Since the absorption spectra of exciplex and free radical ions practically coincide, the straightforward conclusion on the mechanism of radical ion formation by analyzing only TG spectra is impossible. However, the comparison of the fluorescence kinetics of exciplex with the dynamics of TG spectra allows revealing the nature of the primary product of electron transfer (exciplex or solvent-separated ion pair).

In the systems studied, exciplexes occur in equilibrium with excited acceptor molecules as a result of the low value of the Gibbs energy of formation ΔG_{Ex}^* ($-(3-14) \text{ kJ/mol}$ [9, 25]). Therefore, the change in the concentration of the acceptor excited state is described by the sum of two exponents, and that of the exciplex is described by the difference of the same exponents [22]. The comparison of the dynamics of the TG spectra intensities at the wavelengths corresponding to ${}^1\text{CP}^*$ (647 and 492 nm) and to the CP-12DMB exciplex (462 nm) with the fluorescence kinetics of this exciplex shows that they are described by the same rate equations with identical parameters (Fig. 5). This finding proves that the primary product of electron transfer in the CP-12DMB system is the exciplex independent of solvent polarity, while free radical ions are formed in polar solvents as a result of exciplex dissociation. It should be borne in mind that the formation of free radical during the time interval shorter than 5 ns ions cannot contribute significantly to the TG spectrum intensity at $\lambda = 462 \text{ nm}$.

The quantum yield of the radical ion formation from exciplex ϕ_{R}^0 is defined by the expression $\phi_{\text{R}}^0 = \phi_{\text{R}} / (1 - \phi_{\text{f}} / \phi_{\text{f}}^0)$, where ϕ_{f}^0 and ϕ_{f} are the quantum yields of CP fluorescence in the absence and in the presence of a quencher, respectively. The values of ϕ_{R} , ϕ_{R}^0 and the rate constants of the radical ion formation from exciplex $k_{\text{R}}' = \phi_{\text{R}}^0 / \tau_0'$ are listed in Table 1. One can see that the values of k_{R}' depend on ΔG_{et}^* of a donor-acceptor system and, in general, are higher in MeCN than in PrCN. The observed decrease in k_{R}' with an increase in ΔG_{et}^* was qualitatively accounted for in [4] by the stabilization of exciplexes with an increase in ΔG_{et}^* , which results in an increase in the free energy of the activation of exciplex dissociation into radical ions. It is commonly accepted that the dissociation of the exciplex (contact radical ion pair, CRIP) into radical ions occurs via transient formation of the solvent-separated radical ion pair (SSRIP) [3, 4]:



As shown in [3], the reversibility of the first step can be neglected for solvents with a permittivity of $\epsilon > 20$ (e.g., PrCN and MeCN). In this case, the conversion of the exciplex (CRIP) into SSRIP is the rate-limiting step of the reaction. The principal difference between CRIP and SSRIP is primarily in the value of the H_{12} matrix element of electronic coupling of a locally excited (LE) state to a charge-transfer (CT) state ($H_{12} > 0.15$ eV for exciplexes, and $H_{12} < 0.05$ eV for solvent-separated pairs). In addition, the interaction of contact and solvent-separated pairs with a solvent can be considered in terms of the continuum model as dipole solvation and ion solvation, respectively [3, 26]:

$$C = (1.44/r^3)(1/\epsilon - 1/\epsilon_0) - 1.44/r_{AD}\epsilon \quad (2)$$

$$= 4.81(1/\epsilon - 1/\epsilon_0) - 2.4/\epsilon,$$

$$U_{SSRIP} \approx \Delta G_{et} - C = E(D^+/D) - E(A/A^-) - C. \quad (3)$$

Here, C is the energy of solvation and the electrostatic interaction of ions; r (≈ 0.3 nm) and r_{AD} (≈ 0.6 nm) are the ionic radius and the distance between the ions centers in the pair, respectively; ϵ and ϵ_0 are the permittivity of a given solvent and the solvent in which the electrochemical potentials were measured, respectively; U_{SSRIP} is the SSRIP energy relative to the ground state; ΔG_{et} is the Gibbs energy of ground-state electron transfer; and $E(D^+/D)$ and $E(A/A^-)$ are the electrochemical potentials of a donor and an acceptor, respectively.

The dependence of $\log(k'_R)$ on ΔG_{et}^* can be rationalized using the model of correlated polarization of a medium and exciplex [10]. One might assume that the difference in the CRIP and SSRIP energies should depend only on the solvent permittivity and weakly depend on the nature of an electron donor and acceptor. However, as ΔG_{et}^* increases, the difference of the energies of the CT and LE states ($H_{22}^0 - H_{11}^0$) does increase. As a result, the degree of charge transfer z in exciplexes and their dipole moment $\mu = z\mu_0$ (μ_0 is the dipole moment of the contact radical ion pair) decrease:

$$\frac{(H_{22}^0 - H_{11}^0)}{H_{12}} = \left[\frac{1}{z} - 1 \right]^{1/2} - \frac{1}{(1/z - 1)^{1/2}} + 2z\mu_0^2/\rho^3 f(\epsilon). \quad (4)$$

The extent of charge transfer is $0 < z < 1$ for exciplexes and $z = 1$ for solvent-separated pairs. According to the model of correlated polarization of exciplex and medium [27], the free energy of exciplex formation from the locally excited state ΔG_{Ex}^* is equal to

$$\Delta G_{Ex}^* = (H_{22}^0 - H_{11}^0) - H_{12}(1/z - 1)^{1/2} + B - z(2 - z)(\mu_0^2/\rho^3)f(\epsilon), \quad (5)$$

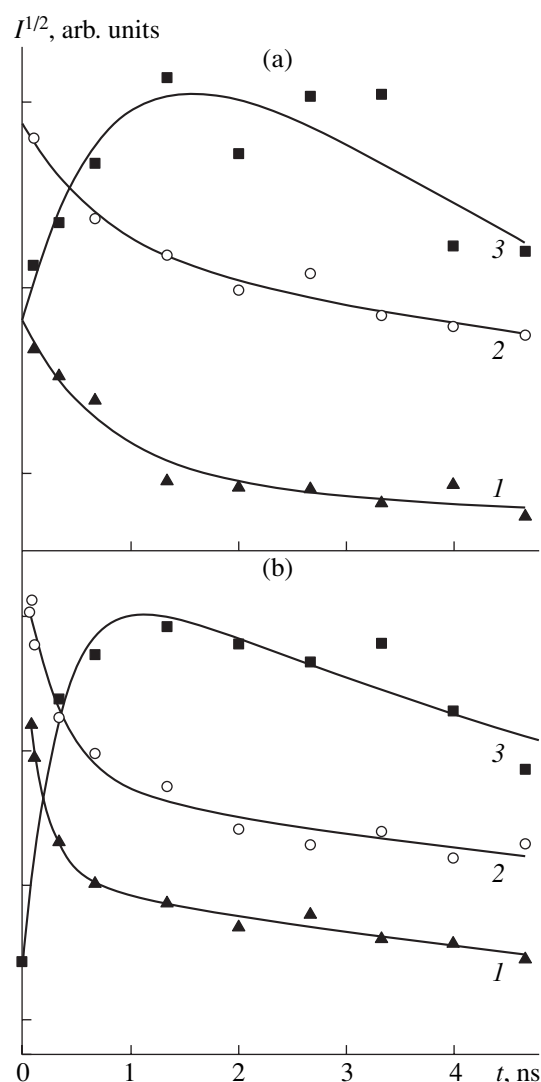


Fig. 5. Dynamics of the TG spectrum intensity for the CP solution in the presence of 12DMB (0.3 mol l^{-1}) in (a) AcOBu and (b) PrCN recorded at 462 (■), 492 (○), and 647 (▲) nm. The values of $I^{1/2}$ at the corresponding wavelength are given, because the intensity of the TG spectra I is proportional to the squared concentration of the product [28]. The calculated curves 1 and 2 refer to the $^1\text{CP}^*$ decay kinetics, and curve 3 corresponds to the formation and decay of the exciplex. The following parameters obtained from the exciplex fluorescence kinetics were used [22]: $\tau_R = 0.3$ ns; $\tau_D = 8$ ns (PrCN) and $\tau_R = 0.8$ ns; $\tau_D = 36$ ns (AcOBu).

where ρ is the radius of the solvent cavity in which the exciplex is located, $f(\epsilon) = (\epsilon - 1)/(2(\epsilon + 2))^2$, and B is the parameter taking account of the entropy of association molecules upon exciplex formation and the repulsion of the reactant molecules. As z decreases, the con-

² As shown earlier, the Lorentz function gives better approximation of the experimental data than the Kirkwood function $f(\epsilon) = (\epsilon - 1)/(2\epsilon + 1)$ [27].

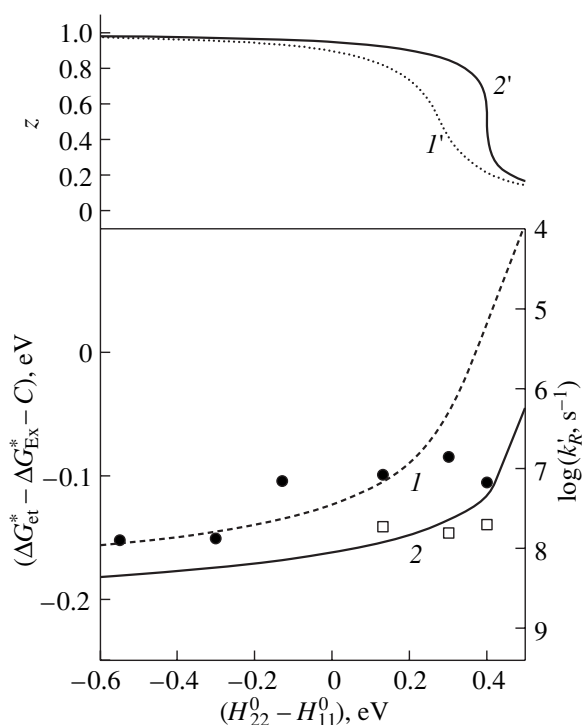


Fig. 6. Plot of $\log(k'_R/s^{-1})$ vs. $(H_{22}^0 - H_{11}^0)$ in PrCN (●) and MeCN (□). Calculated dependences of ΔG_{RI} and z on $(H_{22}^0 - H_{11}^0)$ in (1, 1') PrCN and (2, 2') MeCN.

tribution of the matrix element H_{12} to the exciplex stabilization energy increases [9]. The free energy of the conversion of exciplex (CRIP) into SSRIP can be expressed as:

$$\Delta G_{RI} \approx \Delta G_{et}^* - \Delta G_{Ex}^* - C \approx -0.3 - B + H_{12}(1/z - 1)^{1/2} + z(2 - z)\mu_0^2/\rho^3 f(\epsilon) - C. \quad (6)$$

The energy of SSRIP depends linearly on ΔG_{et}^* , and its value in PrCN exceeds that in MeCN by 0.05 eV. The calculated dependence of ΔG_{RI} and z on $(H_{22}^0 - H_{11}^0)$ in PrCN (curves 1 and 1') and MeCN (curves 2 and 2') are given in Fig. 6. The calculation was carried out with the use of Eqs. (4)–(6) with averaged parameters H_{12} , μ_0^2/ρ^3 , and B for the exciplexes studied earlier [9–11].

One can see that the increase in ΔG_{RI} with an increase in $(H_{22}^0 - H_{11}^0)$ correlates with a decrease in the experimental values of $\log(k'_R)$. The value of k'_R for a given exciplex is lower in PrCN than in MeCN, because the decrease in solvent polarity results in a decrease in z and, hence, an increase in the parameter $H_{12}(1/z - 1)^{1/2}$. In this case, the value of ΔG_{RI} has the higher value in PrCN at the same values of $(H_{22}^0 - H_{11}^0)$ due to the lower magnitude of z (Fig. 6; curves 1', 2'). Thus, the dependence obtained reflects the tendency of the rate of the exciplex dissociation into SSRIP to decrease with an increase in ΔG_{et}^* and a decrease in solvent polarity. This is primarily due to the decrease in z in the exciplex, which results in an increase in the free energy ΔG_{RI} of conversion of CRIP into SSRIP and, consequently, in a decrease in k'_R .

The quantum yields and the rate constants for all processes of the decay of CP-123TMB and CP-135TMB exciplexes are listed in Table 2. The quantum yields (ϕ_f^0) and ϕ_T^0) and the rate constants of fluorescence and intersystem crossing (k'_f , and k'_{isc}) were determined in [1]. The quantum yield of internal conversion in exciplex ϕ'_{ic} was determined from the difference: $\phi'_{ic} = 1 - \phi_f^0 - \phi_T^0 - \phi_R^0$.

Table 2. The quantum yields and the rate constant of fluorescence (ϕ_f^0 and k'_f), intersystem crossing (ϕ_T^0 and k'_{isc}), dissociation into radical ions (ϕ_R^0 and k'_R), and back electron transfer (ϕ'_{ic} and k'_{ic}) for the CP-135TMB and CP-123TMB exciplexes

System	Solvent	τ_0	τ'_0	ϕ_f^0	ϕ_T^0	ϕ_R^0	ϕ'_{ic}	k'_f	k'_{isc}	k'_R	k'_{ic}
		ns						μs^{-1}			
CP-135TMB	PhCH ₃	27	27.4	0.21	0.42	–	0.37	7.7	15.3	–	13.5
	AcOBu	27	32	0.18	0.42	–	0.4	5.6	13	–	12.5
	PrCN	21	14	0.08	0.35	0.2	0.37	5.7	25	14.3	26.4
CP-123TMB	PhCH ₃	27	20	0.21	0.53	–	0.26	10.5	26.5	–	13
	AcOBu	27	6	0.12	0.25	–	0.63	20	41.7	–	105
	PrCN	21	2.3	0.01	0.16	0.18	0.65	4.3	69.6	78.2	283

In the CP-135TMB system with ΔG_{et}^* close to zero, the contributions of the processes of internal conversion, intersystem crossing, and fluorescence in nonpolar solvents are comparable. In PrCN, the quantum yield of fluorescence significantly decreases as a result of the appearance of a new exciplex decay channel, the dissociation into radical ions. However, the contributions of internal conversion and intersystem crossing practically do not vary.

In the CP-123TMB system on the contrary, the contribution of fluorescence and intersystem crossing to the exciplex decay significantly decreases with an increase in solvent polarity, and internal conversion (radiationless back electron transfer in the exciplex) becomes dominating, with the values of k'_{ic} drastically increasing. Note that there is a simultaneous strong increase in k'_{isc} . In fact, the rate constants k'_{isc} and k'_{ic} depend on the solvent polarity and ΔG_{et}^* in similar manners. This problem will be considered in the forthcoming communication.

CONCLUSIONS

The study of time-resolved absorption spectra of transient species on ps, ns, and μs time scales and the fluorescence rise and decay kinetics in donor-acceptor systems with $\Delta G_{\text{et}}^* > -0.1$ eV has allowed us to follow the dynamics of formation and decay of exciplexes and radical ions. On the ps time scale, the absorption spectra of radical anions constitute a part of the absorption spectra of the exciplex generated, whereas the absorption of free radical ions is observed on the μs time scale. A comparison of time changes in radical ion absorption and exciplex fluorescence shows that an exciplex is the only primary species of photoinduced electron transfer, and the radical ions are generated via exciplex dissociation resulting in the complete charge separation. As ΔG_{et}^* decreases, the quantum yields and the rate constants of radical ion formation generally increase. This is the result of an increase in the exoergicity of photoinduced electron transfer. The formation of radical ions from exciplex becomes energetically favorable, thus increasing the efficiency of their formation. The decrease in the rate constants of exciplex dissociation into SSRIP with an increase in ΔG_{et}^* or with a decrease in solvent polarity is caused by a decrease in the degree of charge transfer in the exciplex. In addition to the exciplex dissociation of into radical ions, intersystem crossing and internal conversion (back electron transfer) are the main pathways of exciplex decay. Our results show that the role of radiationless back electron transfer becomes more important and the rate of formation of triplet states increases with an increase in the solvent polarity and a decrease in ΔG_{et}^* . This is due to a decrease in the energy gap between the exciplex and

the triplet state for k'_{isc} and between the exciplex and the ground state for k'_{ic} .

ACKNOWLEDGMENTS

This work was supported by the Russian Foundation for Basic Research, project nos. 02-03-32797, 02-03-32441, and 03-03-33134; the Program of the Russian Federation Ministry of Education and Sciences "Russian Universities," grant no. UR.05.01.002; and the INTAS Foundation, grant no. 00-0772.

REFERENCES

1. Dogadkin, D.N., Dolotova, E.V., Soboleva, I.V., Kuzmin, M.G., Plyusnin, V.F., Pozdnyakov, I.P., Grivin, V.P., Fillips, D., and Murphy, K., *Khim. Vys. Energ.*, 2004, vol. 38, no. 6, p. 434 [*High Energy Chem. (Engl. transl.)*, 2004, vol. 38, no. 6, p. 386].
2. Weller, A., *Z. Phys. Chem. NF*, 1982, vol. 133, no. 1, p. 93.
3. Gould, I.R. and Farid, S., *Acc. Chem. Res.*, 1996, vol. 29, no. 11, p. 522.
4. Vauthey, E., Hogemann, C., and Allonas, X., *J. Phys. Chem. A*, 1998, vol. 102, no. 38, p. 7362.
5. Weinstein, Yu.A., Sadovskii, N.A., and Kuz'min, M.G., *Khim. Vys. Energ.*, 1994, vol. 28, no. 3, p. 244 [*High Energy Chem. (Engl. transl.)*, 1994, vol. 28, no. 3, p. 211].
6. Kikuchi, K., Takahashi, Y., Katagiri, T., Niwa, T., Hoshi, M., and Miyashi, T.A., *Chem. Phys. Lett.*, 1991, vol. 180, no. 5, p. 403.
7. Kuzmin, M.G., *J. Photochem. Photobiol. A: Chemistry*, 1996, vol. 102, no. 1, p. 51.
8. Sadovskii, N.A., Kuzmin, M.G., Gorner, H., and Schaffner, K., *Chem. Phys. Lett.*, 1998, p. 282.
9. Dolotova, E.V., Soboleva, I.V., and Kuz'min, M.G., *Khim. Vys. Energ.*, 2002, vol. 36, no. 1, p. 34 [*High Energy Chem. (Engl. transl.)*, 2002, vol. 36, no. 1, p. 31].
10. Dogadkin, D.N., Soboleva, I.V., and Kuz'min, M.G., *Khim. Vys. Energ.*, 2001, vol. 35, no. 2, p. 130 [*High Energy Chem. (Engl. transl.)*, 2001, vol. 35, no. 2, p. 107].
11. Dogadkin, D.N., Soboleva, I.V., and Kuz'min, M.G., *Khim. Vys. Energ.*, 2001, vol. 35, no. 4, p. 283 [*High Energy Chem. (Engl. transl.)*, 2001, vol. 35, no. 4, p. 251].
12. Vauthey, E. and Henseler, A., *J. Photochem. Photobiol. A*, 1998, vol. 112, no. 1, p. 103.
13. Von Raumer, M., Suppan, P., and Jacques, P., *J. Photochem. Photobiol. A: Chem.*, 1997, vol. 105, no. 1, p. 21.
14. Henseler, A. and Vauthey, E., *J. Photochem. Photobiol. A: Chem.*, 1995, vol. 91, no. 1, p. 7.
14. Grivin, V.P., Khmelinski, I.V., Plyusnin, V.F., Blinov, I.I., and Balashev, K.P., *J. Photochem. Photobiol. A*, 1990, vol. 51, no. 2, p. 167.
15. Tretyakov, E.V., Samoilo, R.I., Ivanov, Yu.V., Plyusnin, V.F., Pashchenko, S.V., and Vasilevsky, S.F., *Mendelev Commun.*, 1999, vol. 9, no. 3, p. 92.

16. Plyusnin, V.F., Ivanov, Yu.V., Grivin, V.P., Vorobjev, D.Yu., Larionov, S.V., Maksimov, A.M., Platonov, V.E., Tkachenko, N.V., and Lemmetyinen, H., *Chem. Phys. Lett.*, 2000, vol. 325, nos. 1–3, p. 153.
17. Compton, R.H., Grattan, T.V., and Morrow, T., *J. Photochem.*, 1980, vol. 14, p. 61.
18. Okada, T., Kida, K., and Mataga, N., *Chem. Phys. Lett.*, 1982, vol. 88, p. 157.
19. Shida, T., *Electronic Absorption Spectra of Radical Ions*, Amsterdam: Elsevier, 1988.
20. Dolotova, E., Dogadkin, D., Soboleva, I., Kuzmin, M., Nicolet, O., and Vauthey, E., *Chem. Phys. Lett.*, 2003, vol. 380, p. 729.
21. *J.B. Birks. Photophysics of Aromatic Molecules*, New York: Wiley, 1970, p. 345.
22. O'Neill, P., Steenken, S., and Schulte-Frohlinde, D., *J. Phys. Chem.*, 1975, vol. 79, no. 25, p. 2773.
23. Murov, S.L., *Handbook of Photochemistry*, New York: Marcel Dekker, 1973.
24. Dogadkin, D.N., Soboleva, I.V., and Kuz'min, M.G., *Khim. Vys. Energ.*, 2002, vol. 36, no. 6, p. 422 [*High Energy Chem.* (Engl. transl.), 2002, vol. 36, no. 6, p. 383].
25. Schweitzer, C., Mehrdad, Z., Shafii, F., and Schmidt, R., *J. Phys. Chem. A*, 2001, vol. 105, no. 22, p. 5309.
26. Kuz'min, M.G., Dolotova, E.V., and Soboleva, I.V., *Zh. Fiz. Khim.*, 2002, vol. 76, no. 7, p. 1235.
27. Kuz'min, M.G. and Soboleva, I.V., *Zh. Fiz. Khim.*, 2001, vol. 75, no. 3, p. 474.
28. Nicolet, O. and Vauthey, E., *J. Phys. Chem. A*, 2003, vol. 107, no. 31, p. 5894.